Torque Ripple Minimization Technique of Position Sensorless BLDC Motor for Variable Speed Drives

Karthika Mahalingam[1,*] and Nisha Kandencheri Chellaiah Ramji[2]

[1]*Department of Electrical and Electronics Engineering, New Horizon College of Engineering, Bangalore*
[2]*Department of Electronics and Communication Engineering, New Horizon College of Engineering, Bangalore*
E-mail: karthikaganesh16@gmail.com
[*]*Corresponding Author*

Received 26 January 2022; Accepted 26 April 2022;
Publication 16 May 2023

Abstract

Brushless Direct Current (BLDC) motors are advantageous because of their higher efficiency, higher speed operations and higher power density. Industrial applications demand BLDC motors free from torque ripple. The torque ripple is due to the unequal commutation period between the energised phase and unenergized phase current. It is a perilous problem in sensorless BLDC drive as it leads to speed oscillations, acoustic noise, serious faults, and vibration in machines. The torque ripple can be reduced either by improving motor design parameter or by improving the motor control strategy. This paper proposes a Proportional Integral (PI) controller-based control scheme for a cuk converter driven sensorless BLDC motor to reduce the torque ripple. The proposed scheme invokes Zero Crossing Point (ZCP) detection with back emf sensing approach. The presence of inductor reduces the ripple in the

Distributed Generation & Alternative Energy Journal, Vol. 38_4, 1255–1278.
doi: 10.13052/dgaej2156-3306.3848

input and output currents. The performance of the strategy is verified using MATLAB R2018a Simulink for different operating conditions of a BLDC drive and the results prove that the recommended scheme decreases the torque ripple compared to the conventional scheme.

Keywords: Sensorless BLDC motor, cuk converter, back emf sensing, torque ripple reduction, PI controller.

1 Introduction

The BLDC motors are best suited for industrial applications due to their merits over traditional brushed motors. The merits of BLDC motor include high efficiency, higher speed operations, high reliability, no commutator and brushes, less maintenance, long operating period, high power density, efficient speed-torque characteristics, good dynamic response, low rotor inertia and low acoustic noise [1].

The conventional DC motors are plagued with challenges like mechanical friction, noise, creation of electric sparks, interference of radio signals, high manufacturing cost and maintenance issues [2]. The research in BLDC motor mainly focuses on the sensorless control with an objective to minimize the volume, cost and weight of the motor, reduce torque ripple, design a compact and versatile controllers and enhance the system reliability [2]. In a sensorless drive, the instant at which the floating phase terminal voltage matches half the input voltage is used to determine the commutation time. There are various back emf sensing methods mentioned in the literature survey viz., ZCP of back emf sensing, Pulse Width Modulation (PWM) strategies, integration method, third harmonic voltage integration and terminal current sensing [3]. The flux distribution in the air gap generates trapezoidal back emf in the BLDC motor [4]. The ZCP of back emf of the floating phase is used to detect the rotor position. The ZCP detection of weakened phase is effective for medium and high speed ranges than low speed ranges [5]. An inductor is connected to the motor windings for low speed operation of the back emf detection with better performance [6].

The torque ripple minimization is a critical problem in sensorless BLDC drive that leads to speed oscillations, acoustic noise, serious faults and vibration in machines [7]. The mutual torque generates useful ripple than the cogging and reluctance torques [8]. The torque ripple is owing to the difference in the commutation time of the conducting phases [9] and cause serious faults in sensorless motor drive. Due to this fault, BLDC motor

cannot be used in high accuracy servo drive applications, where the speed and position control of the drive system is very important. The difference in commutation time and the fault due to this issue also results in speed ripple, noise, vibrations and produces poor quality of speed-torque characteristics.

Dae-Kyong Kim et al. states that the terminal voltage of BLDC motor is used to compute the PWM to minimize the ripple [10]. The developed method is realised experimentally in an air conditioner compressor controller to reduce the pulsating currents and vibrations of BLDC motor. Three commutation control methods are mentioned for a complete evaluation of commutation torque ripple [11]. A comparative analysis of different converter topologies for torque ripple reduction techniques of sensor BLDC is discussed [12].

In the sensorless BLDC drive, the control strategies are mainly dependent on the current and torque control [13]. The hysteresis controllers suffer by several transformations which complicates the control techniques without the improvement in the torque control [14]. Several Direct Torque Control (DTC) topologies have been employed in BLDC motor applying conventional [15, 16] and unconventional [17, 18] inverter topologies. This DTC strategy is used to control the torque using 2-phase and 3-phase conduction mode. But the reduction in torque leads to unbalanced switching frequency of inverter switches and high common mode voltage of brushless DC motor which produces common mode current in drives. This common mode current creates electromagnetic interference, affects bearings of the machine, and increase the heating effect of the armature conductors conduit [19]. This approach balances the inverter switching frequencies by producing control signals from the null voltage vectors and it removes the common mode voltage shortcomings. A two-level hysteresis controller is mentioned using three-phase conduction mode to give significance on active voltage vectors [13].

A low-pass filter is presented for the sensorless control of BLDC motor based solar PV system [20] with Sliding Mode Control (SMC). Two control sensors are proposed for the measurement of DC bus voltage and PV current. This increases the overall system reliability with low cost and less sensors. This technique is experimentally tested in a compressor of cooling system. The rotor position during commutation can be estimated using the flux linkage method [21]. It is stated that the commutation appears at lowest or highest point of flux linkage. This method gives reduction in torque ripple and precise commutation time. A speed independent flux linkage strategy for low speed operation and a novel PI controller for commutation point detection is suggested for high speed operations [22]. This strategy subjected to high

frequency interference, changes in the parameters during starting period and load disturbances.

This paper suggests a PI controller tuning of cuk converter for the torque ripple reduction in a sensorless BLDC motor and uses ZCP detection method of back emf sensing approach for variable speed drives. The proposed strategy performance is verified using MATLAB Simulink with different speed and torque conditions of a BLDC drive. The simulation result shows that the recommended scheme decreases the torque ripple rather than the conventional scheme. The proposed system improves the stability of the BLDC drive and reduces the switching losses. The presence of inductor reduces the input and output current ripple.

2 Mathematical Modelling of BLDC Motor

The schematic circuit of a BLDC motor is shown in Figure 1. In the BLDC motor 2-phases are energised and one phase is non-commutated phase. The stator winding phase resistances are assumed as $R_a = R_b = R_c$ and the self-inductances (L) and mutual inductances (M) are constant [23].

The terminal voltages of three phase BLDC motor are given by,

$$V_a = R_a i_a + L\frac{di_a}{dt} + e_a + U_N \tag{1}$$

$$V_b = R_a i_b + L\frac{di_b}{dt} + e_b + U_N \tag{2}$$

$$V_c = R_a i_c + L\frac{di_c}{dt} + e_c + U_N \tag{3}$$

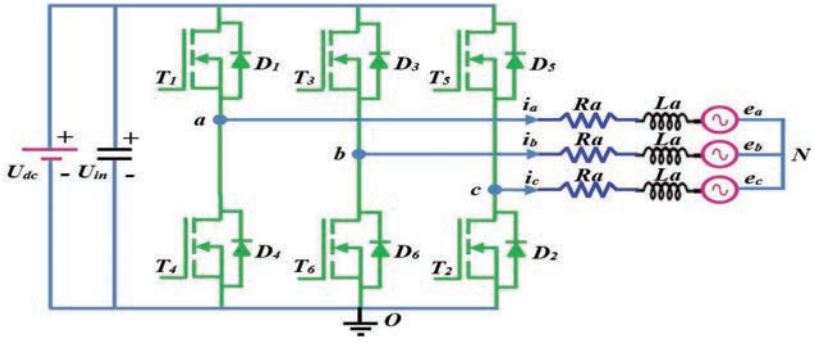

Figure 1 Schematic circuit of BLDC motor.

Where,

$V_a, V_b, V_c =$ Terminal voltages of stator windings in Volts
$i_a, i_b, i_c =$ Phase currents in Ampere
$e_a, e_b, e_c =$ Back emfs in Volts
$L =$Phase inductance in mH
$U_N =$ Neutral point voltage of the motor

We know that under balanced condition,

$$i_a + i_b + i_c = 0$$

$$\begin{bmatrix} V_{ab} \\ V_{bc} \\ V_{ca} \end{bmatrix} = \begin{bmatrix} R_a & 0 & 0 \\ 0 & R_a & 0 \\ 0 & 0 & R_a \end{bmatrix} \begin{bmatrix} i_a \\ i_b \\ i_c \end{bmatrix} + \frac{d}{dt} \begin{bmatrix} L-M & 0 & 0 \\ 0 & L-M & 0 \\ 0 & 0 & L-M \end{bmatrix} \begin{bmatrix} i_a \\ i_b \\ i_c \end{bmatrix} + \begin{bmatrix} e_a \\ e_b \\ e_c \end{bmatrix} + [U_N] \tag{4}$$

The stator voltage equation is given by,

$$V_{ab} = R_a i_a + (L-M)\frac{di_a}{dt} + e_a + U_N \tag{5}$$

$$V_{bc} = R_a i_b + (L-M)\frac{di_b}{dt} + e_b + U_N \tag{6}$$

$$V_{ca} = R_a i_c + (L-M)\frac{di_c}{dt} + e_c + U_N \tag{7}$$

3 Commutation Torque Ripple Analysis

The output torque T_d of a BLDC motor is determined from the output power P_o and from the mechanical angular velocity ω_m and it is driven by the 120° conduction mode. The electromagnetic torque is given by,

$$T_d = \frac{P_o}{\omega_m}$$

$$T_d = \frac{e_a i_a + e_b i_b + e_c i_c}{\omega} \tag{8}$$

Let us consider i_a, i_b as incoming and outgoing phase currents and i_c as floating phase current.

$$i_a = -i_c; i_b = 0;$$

$$i_a = -i_c = I$$

$$e_a = -e_c = E \tag{9}$$

Before commutation, the expression for the developed torque is,

$$T_d = \frac{-2Ei_c}{\omega} \tag{10}$$

After commutation, the torque expression is given by,

$$T_d = \frac{2Ei_b}{\omega} = \frac{-2Ei_c}{\omega}$$

The expression for the terminal voltages during commutation is given by,

$$R_a i_a + L\frac{di_a}{dt} + E + U_N = 0 \tag{11}$$

$$R_a i_b + L\frac{di_b}{dt} + E + U_N = U_{in} \tag{12}$$

$$R_a i_c + L\frac{di_c}{dt} - E + U_N = (1-d)U_{in} \tag{13}$$

Where,

$d =$ Duty cycle switch
$U_{in} =$ Inverter input voltage in Volts

The addition of Equations (11)–(13) gives,

$$U_N = \frac{(2-d)U_{in} - E}{3} \tag{14}$$

From the Equations (13) and (14).
The change in 'c' phase current is given by,

$$\frac{di_c}{dt} = \frac{(1-2d)U_{in} + 4E - 3R_a i_c}{3L} \tag{15}$$

The duty cycle for the steady state non-commutated phase current can be obtained by equating Equation (15) to zero and can be written as,

$$d = 0.5 + \frac{4E - 3R_a i_c}{2U_{in}} \tag{16}$$

During high-speed region torque ripple can be minimized by possessing the inverter input voltage as,

$$U_{in} \geq 4E - 3R_a i_c. \tag{17}$$

The Equation (17) shows that the torque ripple can be reduced by increasing the DC-link voltage to four times the back emf.

4 Proposed Sensorless Commutation Torque Ripple Reduction Strategy

The idea behind the proposed work is to detect the commutation instant and reduce the torque ripple. The commutation instant is detected using the ZCP detection method of back emf sensing. In this method, the floating phase voltage is compared with virtual ground voltage and the instant at which the floating phase voltage is greater than or equal to the ground voltage, the commutation is initiated. This method of back emf sensing is simple and suitable for variable speed drives [24].

In this section, PI controller tuning of cuk converter for a sensorless BLDC motor for the torque ripple minimization is discussed. The Equation (17) shows that during the commutation period, the torque ripple can be minimized by increasing the DC-link voltage to four times the back emf voltage. Hence, the boost mode operation of cuk converter can be used to increase the potential. The cuk converter has continuous input current and output current, it uses L-C filter which reduces the ripple current, and the bidirectional energy flow increases the efficiency of the converter. Since the voltage of the cuk converter must be increased during commutation, Pulse Amplitude Modulation (PAM) scheme is used to increase the value of DC-link voltage during commutation time.

The cuk converter with PAM provides a sudden increase in the input voltage during commutation than the other type of converters. The boost mode of cuk converter is used to reduce the current ripple during the commutation period. The proposed strategy shown in Figure 2 consists of rotor position sensing unit, phase voltage control unit of converter, non-commutated phase current control unit and mode selection unit of cuk converter. The actual speed and current are adjusted to obtain the voltage control of the cuk converter. This voltage control unit consists of PI speed and current controller to provide the voltage for the MOSFET of cuk converter and based on this voltage, the mode selection unit performs its operation.

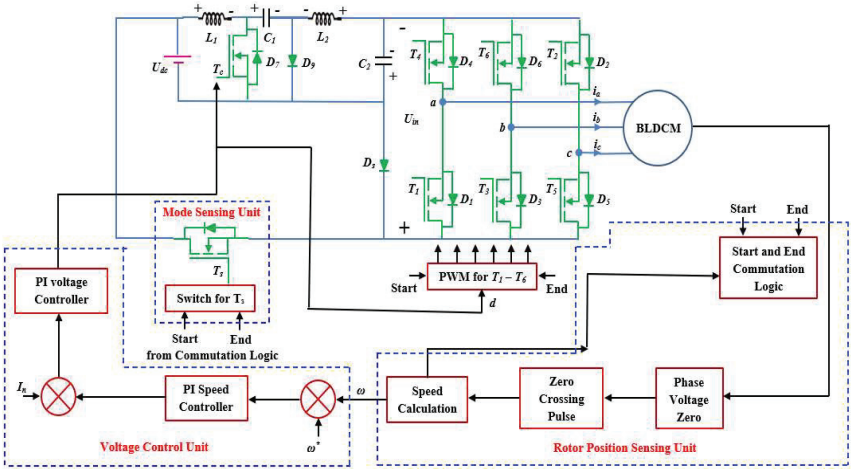

Figure 2 Block diagram of the proposed torque ripple reduction strategy.

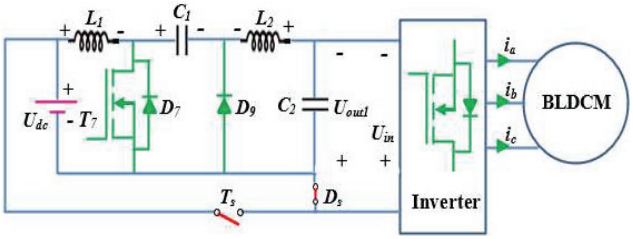

Figure 3 Normal conduction period of cuk converter.

During the buck-boost mode, the inverter and BLDC drive are supplied by the DC voltage and it is increased during the boost mode. The voltage chopping is done by PAM which in turn reduces the voltage stress on MOSFET and reduces the current ripple. The cuk converter shown in Figure 3 is suggested to improve the input voltage during the commutation interval. The switch T_s and diode D_s are used as the mode selection circuit. The normal conduction is enabled by turning off T_s and by turning ON the diode D_s to run the BLDC motor through the DC supply voltage. During this mode of operation, the inverter input voltage can be controlled by the speed and current control strategy without the PWM scheme. At the instant of the normal conduction, the average line voltages of conducting phases are given by the Equations (5) and (7),

$$V_{ac} = -2R_a i_c + 2E = d_n U_{in} \tag{18}$$

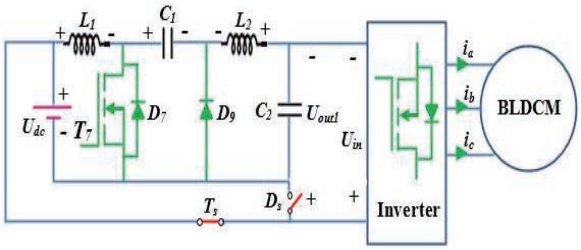

Figure 4 Cuk converter during commutation.

Table 1 Proposed system parameters

Motor Type and Proposed Converter	Parameters	Values
PMBLDC motor	Voltage, V	24 V
	Power, P	70 W
	Rated current, I	4 A
	Rated load Torque, T	2 N/m
	Rated speed, N	3000 r/min
	Back EMF coefficient, k_e	0.028 V/(rad/s)
	Number of poles, p	6
	Resistance, R_{ph}	0.33 Ω
	Inductance, L	0.61 mH
Cuk converter	Capacitance C_1	1100 μF
	Capacitance C_2	2200 μF
	Inductance L_1	330 μH
	Inductance L_2	330 μH

Where,
d_n = Duty cycle of inverter switch T_1

$$d_n = \frac{-2R_a i_c + 2E}{U_{in}} \tag{19}$$

In Figure 4, the switch T_s is closed and diode D_s is open during commutation and the converter is operating in boost mode. In this condition, the DC input voltage is improved by including the capacitor voltage. The proposed strategy performance is verified under rated conditions with the parameters given in the Table 1.

The duty cycle of the cuk converter switch is given by,

$$d_c = \frac{2R_a i_n + 2E}{U_{in} + 2R_a i_n + 2E} \tag{20}$$

The steady state non-commutated phase current control unit is used to maintain steady current and to decrease the ripple. The duty cycle of the MOSFET during commutation period is given by,

$$d = 0.5 + \frac{4E + 3R_a i_n}{2(U_{in} + 2R_a i_n + 2E)} \tag{21}$$

Where,

$i_n =$ unenergised phase current in Ampere
$d =$ Switch T_s duty cycle

The instant at which the commutated phase current becomes zero, the end point of commutation commences and switch T_s turns OFF and the cycle repeats. Equation (21) is used to maintain the constant state of the floating phase current. The torque ripple rate in terms of current ripple rate is given by,

$$I_{ripple} = \frac{I_{max} - I_{min}}{I_{max} + I_{min}} \tag{22}$$

I_{max} and I_{min} are maximum and minimum current ripple for the given period respectively.

This topology has many advantages such as reduction in torque ripple reduction, PAM technique evades the voltage spikes during turn on and off condition of switches and it is a simple modulation scheme.

5 Results and Discussions

The simulation is carried out using MATLAB to justify the robustness of the recommended cuk converter-based torque ripple reduction method under different parameter changes. The analysis of various conditions of load torque and speed are considered to obtain the steady state condition of non-commutated phase current and torque ripple. The details of proposed system parameters are shown in Table 1.

Figure 5 shows the Conventional converter scheme (a) Torque waveform (b) Three-phase stator current (c) DC input voltage (d) and (e) Commutation logic signals of switches T_1 and T_4 of the conventional converter. Figure 6 shows the proposed converter scheme (a) Torque waveform (b) Three-phase stator current (c) DC input voltage (d) and (e) Commutation logic signals of switches T_1 and T_4 of the proposed cuk converter (f) and (g) Gate pulses of switches T_7 and T_s. The ZCP of back emf sensing method is used to find the start/end commutation points. The comparison of conventional PWM control

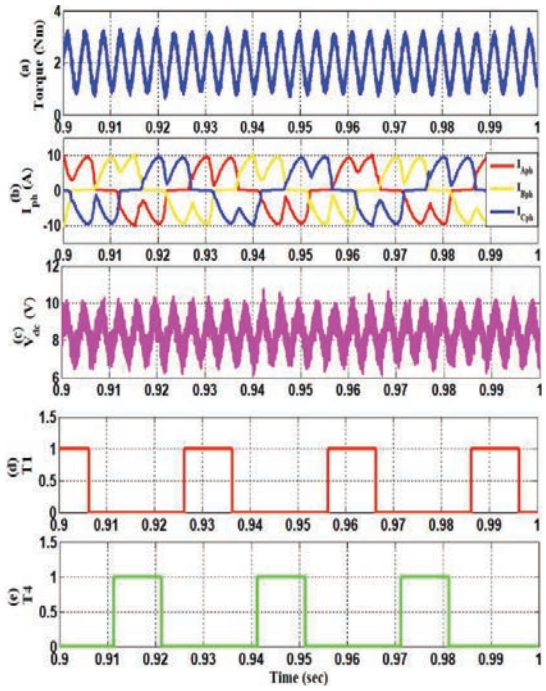

Figure 5 Conventional converter scheme (a) Torque waveform (b) Three-phase stator current (c) DC input voltage (d) and (e) Commutation logic signals of switches T_1 and T_4 of the conventional converter.

method and proposed cuk converter-based PI controller tuning methods are carried out using simulink analysis. The speed and voltage controller gain values are mentioned in Table 2.

The output waveforms of proposed scheme maintain the steady state condition of the floating phase current and reduces significant amount of the current ripple. In the proposed method, both the energised phase currents are alike during commutation and the current is maintained constant by the application of boosted voltage with PAM method. The torque ripple of conventional method is compared with the proposed cuk converter method for the sensorless BLDC drive. The torque ripple can be calculated as,

$$\%\text{Torque ripple} = \frac{T_{mx} - T_{mn}}{T_l} \tag{23}$$

Where,

T_{mx} = Maximum value of instantaneous torque in Nm

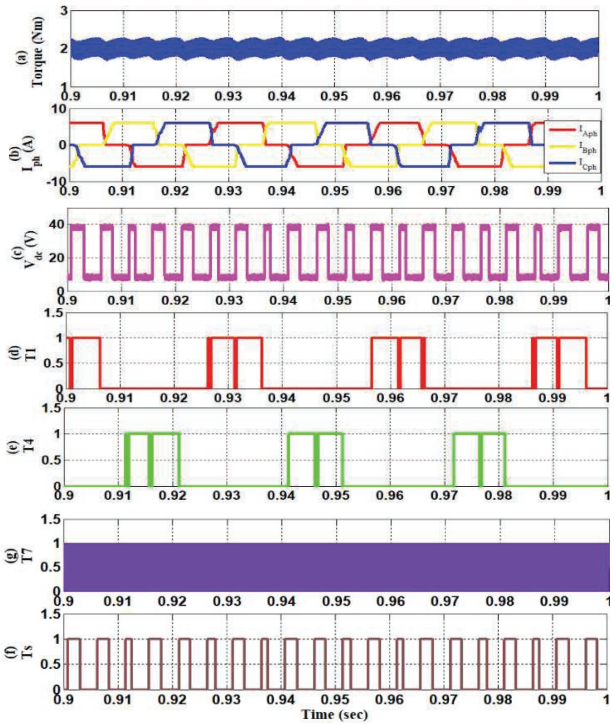

Figure 6 Proposed converter system (a) Torque waveform (b) Three-phase stator current (c) DC input voltage (d) and (e) Commutation logic signals of switches T_1 and T_4 of the proposed cuk converter (f) and (g) Gate pulses of switches T_7 and T_s.

Table 2 Speed and voltage controller gains

	PI Controller Tuning	
Parameters	Proportional Gain K_p	Integral Gain K_i
Speed	0.1	15
Voltage	0.1	0.5

T_{mn} = Minimum value of instantaneous torque in Nm
T_l = Load torque in Nm

In this torque ripple reduction analysis, the following conditions of the load torque and speed are considered to understand the variations in load torque with respect to speed and vice-versa.

Case 1: Constant load torque-low-speed region
Case 2: Constant load torque-high-speed region

Case 3: Variable load torque-Constant speed
Case 4: Variable Speed-Constant load torque

All the above cases the constant load torques of 2 Nm and 5 Nm and variable load torque of 2 Nm to 5 Nm and the constant speed of 500 rpm, 1500 rpm and variable speed of 1300 rpm to 1500 rpm are considered.

Case 1: Constant load torque-low-speed region:

The back emf is minimum during low-speed and the duty cycle is fifty percentage and hence it is not imperative to increase the DC-link voltage under commutation period. It is observed from Equations (20) and (21),

$$d = 2d_c \tag{24}$$

Therefore, during low-speed by applying twice the duty cycle of cuk converter switch, the required voltage can be obtained. In case 1, the constant load torque of 2 Nm with 500 rpm is considered for the traditional and proposed system as shown in Figures 7 and 8.

In the conventional PWM method, the non-commutated phase current ripple is as high as 85.6% for the DC-link voltage of 10V, 10A system whereas the proposed system reduces the ripple to 15% which is 65.6% higher reduction than the conventional method. The proposed method uses PAM to the switches which minimizes the harmonics caused by flick off. This reduces considerable amount of the torque ripple.

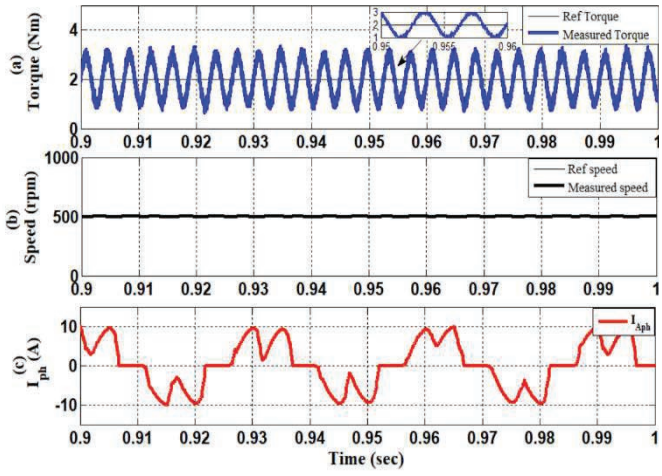

Figure 7 Constant load torque of 2 Nm with 500 rpm of the conventional converter (a) Torque (b) Speed (c) Phase current.

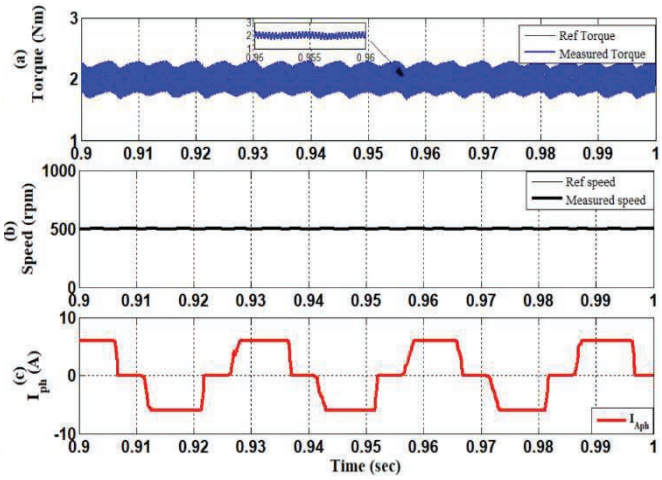

Figure 8 Constant load torque of 2 Nm with 500 rpm of the proposed cuk converter (a) Torque (b) Speed (c) Phase current.

Case 2: Constant load torque-high-speed region:

During high-speed the back emf is high and even for unity duty cycle the required DC voltage has to be increased to decrease the torque ripple under commutation period. Hence, the cuk converter operated in boost mode to increase the voltage during commutation. This can be achieved by modifying the Equation (21) as,

$$d = 0.5 + \frac{4E + 3R_s i_n}{4(U_{in} + 2R_s i_n + 2E)} \tag{25}$$

The inverter voltage can be boosted by PAM method to operate the BLDC motor in high speed.

Figures 9 and 10 shows the case 2 waveforms. The constant load torque of 2 Nm with 1500 rpm is considered for the traditional and proposed system. In the conventional PWM method, the non-commutated phase current ripple is as high as 43.8%. This method reduces the ripple to 6.2%. This percentage of reduction is 37.6% more than the conventional method.

Case 3: Variable load torque-Constant speed:

In case 3, the dynamic performance of the recommended and conventional system has been observed by considering the variable load torque of 5 Nm to 2 Nm with 1500 rpm as shown in Figures 11 and 12. In the conventional PWM method, first the torque is reduced from 5 Nm to 2 Nm at 1 sec

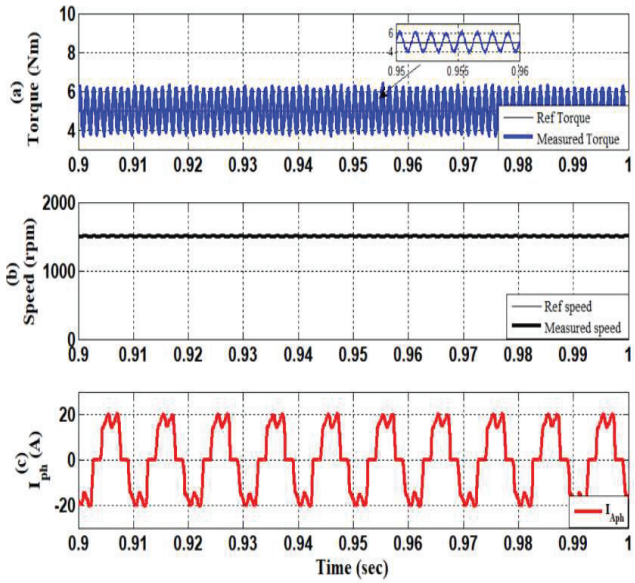

Figure 9 Constant load torque of 5 Nm with 1500 rpm of the conventional converter (a) Torque (b) Speed (c) Phase current.

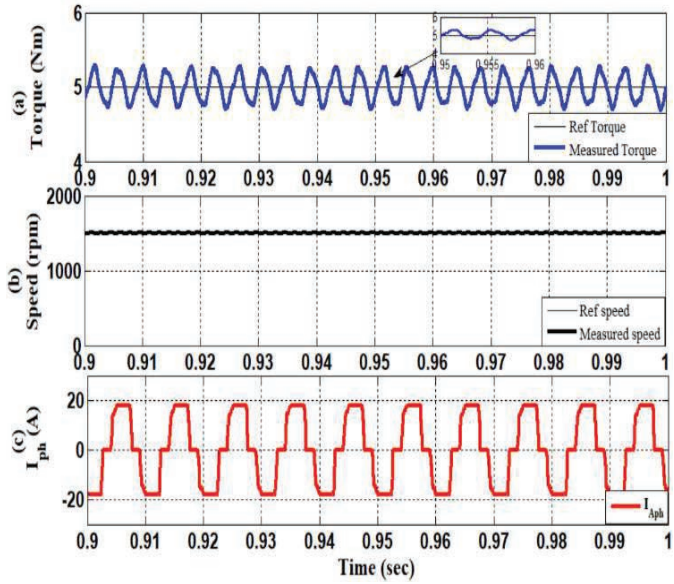

Figure 10 Constant load torque of 5 Nm with 1500 rpm of the proposed cuk converter (a) Torque (b) Speed (c) Phase current.

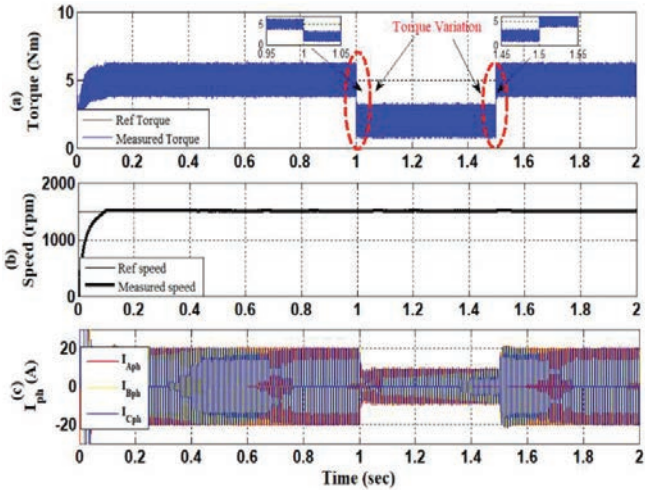

Figure 11 Variable load torque of 5 Nm-2 Nm with 1500 rpm of the conventional converter (a) Torque (b) Speed (c) Phase current.

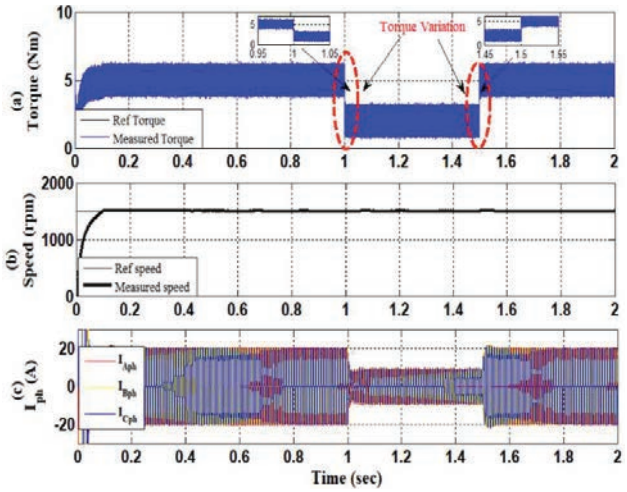

Figure 12 Variable load torque 5 Nm-2 Nm with 1500 rpm of the proposed cuk converter (a) Torque (b) Speed (c) Phase current.

followed by an increment in the torque from 2 Nm to 5 Nm at 1.5 sec. The corresponding variation in the non-commutated phase current ripple and torque ripple are observed as high as 48.4%. During the change in the torque, the voltage is maintained constant and the speed oscillations is less than 1 rpm and it's negligible.

In the proposed scheme for the same condition of change in torque of 5 Nm to 2 Nm at 1 sec and an increment of 2 Nm to 5 Nm at 1.5 sec the torque ripple is reduced to 4.6% to 10% which is comparatively 43.8% reduction than the conventional method. This condition is observed for the DC-link voltage of 45V, 10A system with the small speed oscillations. The variation in non-commutated phase current is comparatively small in the proposed cuk converter method.

Case 4: Variable Speed-Constant load torque:

In case 4, (Figures 13 and 14) the dynamic performance of the proposed and conventional system has been observed by considering the variable speed of 1300 rpm to 1500 rpm and a constant load torque of 5 Nm. In the conventional PWM method, first the speed is increased from 1300 rpm to 1500 rpm at 1 sec followed by a decrement in the speed from 1500 rpm to 1300 rpm at 1.5 sec. The corresponding variation in the non-commutated phase current ripple and torque ripple are observed as high as 32.8%. During the change in the speed, the voltage is maintained constant and the slight variation in torque is negligible.

In the proposed scheme for the same condition of the change in speed from 1300 rpm to 1500 rpm at 1 sec and the change in speed from 1500 rpm at 1 sec to 1300 rpm at 1.5 sec, the torque ripple is reduced to 4.6% which is

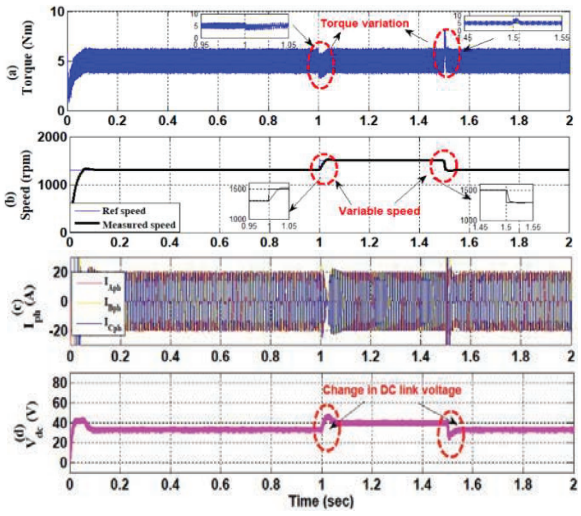

Figure 13 Variable speed of 1500 rpm – 1300 rpm with 5 Nm load torque of the conventional converter (a) Torque (b) Speed (c) Phase current.

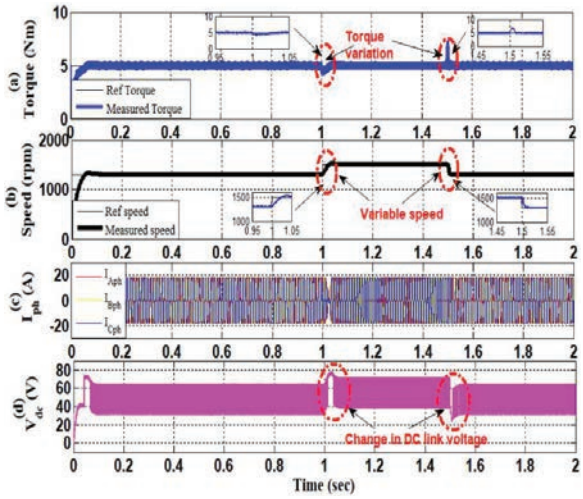

Figure 14 Variable speed of 1500 rpm – 1300 rpm with 5 Nm load torque of the proposed cuk converter (a) Torque (b) Speed (c) Phase current.

Table 3 Comparative analysis of torque ripple reduction

			Conventional Method	Proposed cuk Converter
Different Cases	Load Torque in Nm	Speed in rpm	% Torque Ripple	
Case 1	2	500	85.6%	15%
Case 2	5	1500	43.8%	6.2%
Case 3	2–5	1500	48.4%	10%
Case 4	5	1300–1500	32.8%	4.6%

comparatively 28.2% reduction than the conventional method. This condition is observed for the DC-link voltage of 45V, 10A system. It is detected that a fleeting torque spike is produced and abridged swiftly with the small speed oscillations. The variation in non-commutated phase current is comparatively small in the proposed cuk converter method.

The Table 3 shows comparative analysis of the torque ripple reduction of conventional and proposed scheme.

The drive system is tested for all four cases, and it is evident from the table that the proposed strategy reduces the torque ripple considerably. While the reduction in torque ripple is significant in both ranges under constant load torque condition, it is equally appreciable in the other two cases thus proving the merit of the proposed strategy. During constant torque-low speed

condition the torque ripple is found to be 15% whereas it stands at 6.2% during for the high-speed region. Similarly, the ripple is reduced by almost 38.4% for the variable torque condition and for the variable speed condition the percentage reduction is found to be 28.2%.

6 Conclusion

The proposed strategy achieves a significant reduction in torque ripple through a PI controller tuned cuk converter for a sensorless BLDC motor. The performance of the strategy is verified using MATLAB R2018a Simulink for different operating conditions of a BLDC drive. The ZCP detection combined with cuk converter improves the input voltage during the commutation interval. The converter is operated in boost mode during commutation, and the DC input voltage is increased by adding the capacitor voltage. The simulation results conclude that there is a reduction in torque ripple compared to the conventional scheme under all the four operating conditions. It is observed that the reduction is 15% during constant torque-low speed condition whereas 6.2% reduction is achieved in the high-speed region. Similarly, the reduction is 10% for the variable torque condition period and it is 4.6% during variable speed condition. The proposed strategy improves the stability of the system as it reduces the torque ripple and improves the efficiency due to PAM technique and bidirectional energy flow. Validation of simulation results with an indigenous hardware arrangement is considered as the future scope of this work.

References

[1] B. Singh and S. Singh, "State of the art on permanent magnet brushless DC motor drives," *J. Power Electron.*, vol. 9, no. 1, pp. 1–17, 2009.

[2] C. L. Xia, *Permanent Magnet Brushless DC Motor Drives and Controls*. 2012.

[3] T. H. Kim and M. Ehsani, "Sensorless control of the BLDC motors from near-zero to high speeds," *IEEE Trans. Power Electron.*, vol. 19, no. 6, pp. 1635–1645, 2004.

[4] "8 Sensorless TR commutation tech 2006 (2).pdf." .

[5] B. Hu, J. Lee, S. Sathiakumar, and Y. Shrivastava, "A novel sensorless algorithm of the trapezoidal back-electromagnetic force brushless DC motors from near-zero to high speeds," *Aust. J. Electr. Electron. Eng.*, vol. 9, no. 3, pp. 263–274, 2012.

[6] M. N. Eskander, O. M. Arafa, and O. A. Mahgoub, "Sensorless control of PMSM and BDCM based on EMF extraction and extended kalman estimator," *IEEE Int. Symp. Ind. Electron.*, vol. 3, pp. 2168–2175, 2006.

[7] Z. Li, Q. Kong, S. Cheng, and J. Liu, "Torque ripple suppression of brushless DC motor drives using an alternating two-phase and three-phase conduction mode," *IET Power Electron.*, vol. 13, no. 8, pp. 1622–1629, 2020.

[8] G. Liu, S. Chen, S. Zheng, and X. Song, "Sensorless Low-Current Start-Up Strategy of 100-kW BLDC Motor with Small Inductance," *IEEE Trans. Ind. Informatics*, vol. 13, no. 3, pp. 1131–1140, 2017.

[9] G. Liu, C. Cui, K. Wang, B. Han, and S. Zheng, "Sensorless Control for High-Speed Brushless DC Motor Based on the Line-to-Line Back EMF," *IEEE Trans. Power Electron.*, vol. 31, no. 7, pp. 4669–4683, 2016.

[10] D. K. Kim, K. W. Lee, and B. Il Kwon, "Commutation torque ripple reduction in a position sensorless brushless dc motor drive," *IEEE Trans. Power Electron.*, vol. 21, no. 6, pp. 1762–1768, 2006.

[11] S. Y. Jung, Y. J. Kim, J. Jae, and J. Kim, "Commutation control for the low-commutation torque ripple in the position sensorless drive of the low-voltage brushless DC motor," *IEEE Trans. Power Electron.*, vol. 29, no. 11, pp. 5983–5994, 2014.

[12] K. Mahalingam, N. Kandencheri, and C. Ramji, "A comparative analysis of torque ripple reduction techniques for sensor BLDC drive," vol. 13, no. 1, pp. 122–131, 2022.

[13] M. Masmoudi, B. El Badsi, and A. Masmoudi, "Direct torque control of brushless DC motor drives with improved reliability," *IEEE Trans. Ind. Appl.*, vol. 50, no. 6, pp. 3744–3753, 2014.

[14] S. J. Park, H. W. Park, M. H. Lee, and F. Harashima, "A new approach for minimum-torque-ripple maximum-efficiency control of BLDC motor," *IEEE Trans. Ind. Electron.*, vol. 47, no. 1, pp. 109–114, 2000.

[15] Y. Liu, Z. Q. Zhu, and D. Howe, "Direct torque control of brushless DC drives with reduced torque ripple," *IEEE Trans. Ind. Appl.*, vol. 41, no. 2, pp. 599–608, 2005.

[16] Z. Q. Zhu and J. H. Leong, "Analysis and mitigation of torsional vibration of PM brushless AC/DC drives with direct torque controller," *IEEE Trans. Ind. Appl.*, vol. 48, no. 4, pp. 1296–1306, 2012.

[17] S. B. Ozturk, W. C. Alexander, and H. A. Toliyat, "Direct torque control of four-switch brushless dc motor with non-sinusoidal back emf," *IEEE Trans. Power Electron.*, vol. 25, no. 2, pp. 263–271, 2010.

[18] M. Masmoudi, B. El Badsi, and A. Masmoudi, "DTC of B4-inverter-fed BLDC motor drives with reduced torque ripple during sector-to-sector commutations," *IEEE Trans. Power Electron.*, vol. 29, no. 9, 2014.

[19] G. Oriti, A. L. Julian, and T. A. Lipo, "Inverter/motor drive with common mode voltage elimination," *Conf. Rec. – IAS Annu. Meet. (IEEE Ind. Appl. Soc.*, vol. 1, pp. 587–592, 1997.

[20] M. Dubey, S. K. Sharma, and R. Saxena, "Solar power-driven position sensorless control of permanent magnet brushless DC motor for refrigeration plant," *Int. Trans. Electr. Energy Syst.*, vol. 30, no. 7, pp. 1–15, 2020.

[21] M. Jafarboland and M. H. R. Silabi, "New sensorless commutation method for BLDC motors based on the line-to-line flux linkage theory," *IET Electr. Power Appl.*, vol. 13, no. 6, pp. 757–765, 2019.

[22] S. Chen, G. Liu, and L. Zhu, "Sensorless Control Strategy of a 315 kW High-Speed BLDC Motor Based on a Speed-Independent Flux Linkage Function," *IEEE Trans. Ind. Electron.*, vol. 64, no. 11, pp. 8607–8617, 2017.

[23] M. Karthika and K. C. R. Nisha, "Review on Torque Ripple Reduction Techniques of BLDC Motor," in *2020 International Conference on Inventive Computation Technologies (ICICT)*, 2020, pp. 1092–1096.

[24] Q. Wang, S. Wang, and C. Chen, "Review of sensorless control techniques for PMSM drives," *IEEJ Trans. Electr. Electron. Eng.*, vol. 14, no. 10, pp. 1543–1552, 2019.

Biographies

Karthika Mahalingam received her B.E degree in Electrical and Electronics Engineering from M K university, Madurai in 2002. She received M.E in Power Electronics and drives from Anna university in 2012. She is working as a senior Assistant professor in Department of Electrical and Electronics Engineering, New Horizon College of Engineering, Bangalore. Currently, she is pursuing Ph.D in New Horizon College of Engineering, Bangalore, Visvesvaraya Technological University, Belagavi, Karnataka, India. Her research interest includes BLDC drives, Power Electronics controllers, and Renewable energy sources.

Nisha Kandencheri Chellaiah Ramji received her B.E degree in Electronics and Communication Engineering from Bharathidasan University, Trichy in 2002. She received M.E in Power Electronics and Ph.D in Power Converters for Renewable Energy Systems from Sathyabama University, Chennai in 2004 and 2015 respectively. She started her career as lecturer in Sathyabama University (2003–2009). She joined New Horizon College of Engineering, Bangalore, Visvesvaraya Technological University, Belagavi, Karnataka,

India in 2009 and currently working as a Professor at the Department of Electronics and Communication Engineering. She has more than 16 years of academic cum research experience at university and college level. Her contributions are accorded in the field of efficient Power Converters for Renewable Energy systems and Embedded control of Power applications.